Chapter 4

REAL-TIME SIMULATION OF VARIATIONAL MODE DECOMPOSITION METHOD FOR ISLANDING DETECTION

4.1 INTRODUCTION

Ascertaining unintentional islanding conditions is a challenging task for power utility operators due to the pervasive penetration of distributed energy resources (DER). The presence of DER has a significant adverse impact on islanding detection schemes for various types of distributed generators (DG) and inverters. This chapter addresses the passive islanding detection mechanism based on mode energy index using variational mode decomposition (VMD) in an active distribution network. The prime attributes of VMD are noise immunity, robustness, and non-recursive signal processing approaches, making it more promising and competent for signal decomposition than other extant signal processing methods. In this chapter, three-phase instantaneous voltages at the targeted DG end have been acquired to compute modal voltage signals, and VMD has been applied to decompose the obtained signals into four modes. Thereupon, the mode energy index has been calculated for the selected mode. The estimated energy index has ultimately been utilized as an islanding detection indicator. This work has modeled two different test systems, and test data has been simulated using EMTDC/PSCAD. The simulation outcomes reassert that the developed approach effectively ascertains the islanding and non-islanding. Furthermore, the proposed islanding detection technique has been validated using the Real-Time Digital Simulator (RTDS) platform.

The chapter's contribution can be summarized as follows:

- A fast and straightforward IDT using a modal voltage signal has been presented. The islanding/non-islanding condition has been decided without directly impacting the system operation.
- The proposed method is well competent in ascertaining the islanding within 0.11s in the case of a zero power deficit.
- The proposed method's real-time simulation and validation have been carried out on the RTDS/RSCAD and dSPACE platform to reaffirm its efficacy and feasibility.

The proposed IDT can discriminate between non-islanding and islanding events under extreme system operating conditions such as noise, sag, swell, etc. The remaining of this chapter is organized as follows: Section 4.2 elaborates on the proposed IDT. The description of simulated test systems, results, and discussion are given in Section 4.3. Comparative analysis with the existing methods is discussed in Section 4.4. Real-time simulation validation is illustrated in Section 4.5, followed by the conclusion in Section 4.6

4.2 PROPOSED ISLANDING DETECTION TECHNIQUE DESCRIPTION

The conceptual overview of the proposed IDT has been given in this section. Proposed IDT utilizes Mode Energy (ME) which is computed from the decomposed modal voltage signal at the targeted DER. The flowchart of the proposed islanding detection algorithm has been depicted in Figure 4.1. Initially, VMD has been applied to decompose the multi-component input voltage signal into the modes with their specific central frequency. After acquiring the modes, their energy has been calculated. Ultimately, the ME index is

compared with a predefined threshold for ascertaining the islanding and non-islanding events.

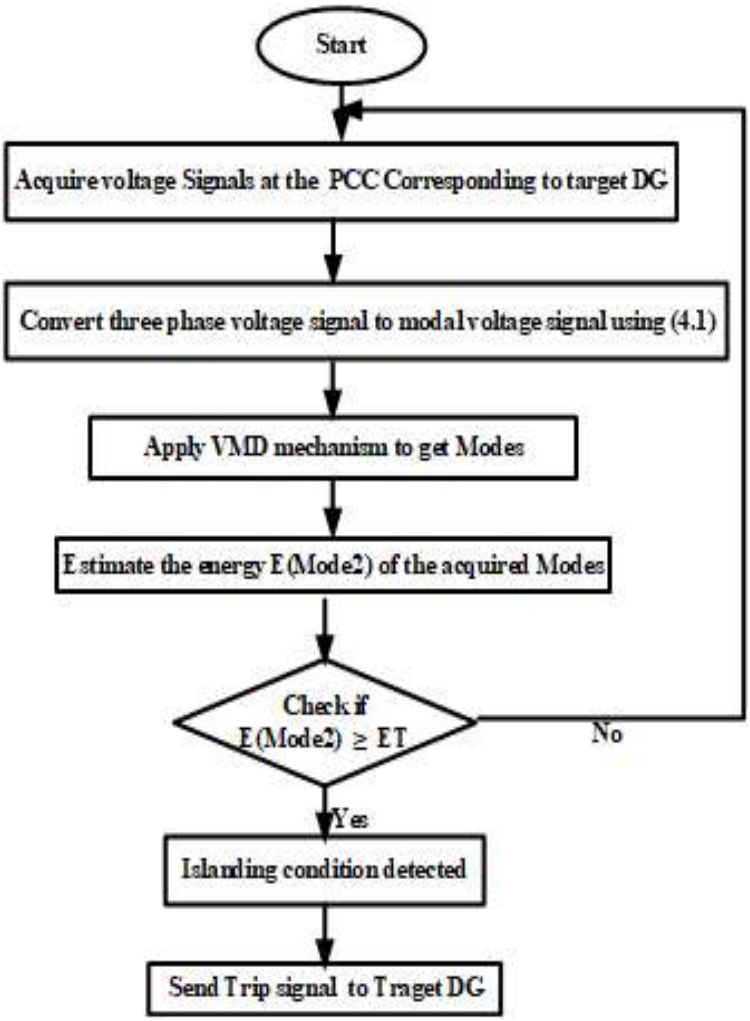

Figure 4.1 Flow chart of Proposed Scheme for Islanding Detection

4.2.1 Modal Voltage Signal

The modal signal transformation is obtained from three-phase instantaneous voltages without canceling each phase's transients. It reduces the processing time and memory requirements making the algorithm efficient. The modal signal has been constructed by a proper linear combination of the three-phase current or voltage signals as given in 4.1.

$$V_m = a_1 V_a + a_2 V_b + a_3 V_c \quad (4.1)$$

where, V_m is the modal voltage signal; V_a ,V_b and V_c are the instantaneous phase voltages; a_1 , a_2 and a_3 are the linear coefficient of the modal signal. It should preserve transient information of the original signal. The values of the modal coefficients are $1, 2,$ and -3 taken from [60].

4.2.2 VMD

VMD is an adaptive and non-recursive method for decomposing a non-stationary signal into a band-limited intrinsic mode function [92]. A real-valued signal $X(t)$ has been decomposed into finite number of modes (sub-signal)/ Intrinsic Mode Function (IMF) to exploit sparsity feature while reconstructing the input signal, $X(t)$ represented in (4.2).

The input modal voltage signal feature has been preserved into the decomposed modes and is used for islanding detection. In VMD, modes are extracted concurrently, which is different from similar methods such as EMD and Wavelet, where the recursive approach is used to extract particular frequency components in the time domain. The capability of computing modes concurrently makes VMD faster as compared to wavelet and EMD based methods. $f_m(t)$ is defined as amplitude and frequency modulated sub-signal with sinusoidal behavior and known as mode/IMF.

$$X(t) = \sum_{m=1}^{M} X_m(t) = \sum_{m=1}^{M} A_m(t)\cos\left(\phi_m(t)\right) \quad (4.2)$$

Where $X(t)$ is the original signal. $X_m(t)$ is a mode of the decomposed signal. $A_m(t)$ is the amplitude envelope of the mode. ϕ_m is the phase of mode. And $\omega_m(t) = \phi'_m(t)$ is defined as the instantaneous frequency.

A detailed discussion on VMD has been presented in the previous chapter 3.

4.2.3 Selection of Mode for energy calculation

The acquired four modes have different frequencies in which the first mode contains the signal's fundamental frequency component. The mode2 contains intermediate frequencies that appear during the transients, such as Islanding. Mode3 and Mode4 contain high-frequency signals that appear in the case of transients arising due to the switching of capacitors and faults. Therefore, mode2 has been chosen in the proposed technique for calculating the values of mode energy index for islanding detection.

4.2.4 Mode Energy (ME) index calculation

The mode energy has been calculated for the quantitative and qualitative analysis of power disturbance events to distinguish between islanding and non-islanding events. The acquired decomposed modes have different components of frequencies. After the signals' decomposition, the specific mode's energy is computed using equation (4.3). The mode energy has been compared with the predefined Energy threshold (ET) to detect islanding events.

$$ME = E(mode_m) = \sum_{k=0}^{K-1} |mode(k)|^2 \qquad 4.3$$

Here $E(mode_m)$ represents mode energy, sample length of mode is defined as K. As many as 64 samples per cycle have been considered for energy calculation.

4.2.5 Computational Burden

This is an essential parameter for the signal processing-based methods. A comparative analysis of the computational burden of the proposed VMD and other available frequency-based decomposition techniques has been presented in Table 4-1. The analysis has been performed on a Desktop featuring Processor Intel(R) Core(TM) i7-8700 CPU @ 3.20GHz and Installed RAM 32.0 GB (31.8 GB usable) using MATLAB 2017B. The data sample size (4096) and the number of decomposed modes (M=4) are the same for comparison. It can be clearly seen that VMD has a better time response than the other signal decomposition methods available in the literature.

Table 4-1 Comparison of Computational Burden

Decomposition Method	Computational Time(s)
EMD	0.115244
EEMD	0.220097
TVF-EMD	0.454084
EWT	0.140373
VMD	0.099729

4.3 SIMULATION RESULTS AND DISCUSSION

The test systems have been modeled in PSCAD/EMTDC environment. Various islanding and non-islanding scenarios have been simulated, and the PCC voltage data has been stored for the analysis of the proposed IDT. The proposed method has been implemented

in MATLAB 2017b on a personal computer. The voltage waveform has been sampled with a 4 kHz sampling frequency.

4.3.1 Test system I:

In Figure 4.2, the single line diagram of the simulated Test system-I has been represented. The test system with a 132 kV substation contains 100 MVA,132/33 kV step-down transformer. At bus5, 30 MVA DG set is connected with a 33/0.69 kV transformer. Wind DG(DFIG) and Synchronous DG set of 5 MVA have been connected with a 33/0.69 kV transformer. The loads are connected at bus3 and bus5. The load, transformer, distribution line, and DG parameters have been taken from the appendix. Various events with varying scenarios have been simulated. The different types of load-shedding have been considered as reported in [99]. The voltage waveform of the target DG has been captured and stored for further analysis. Table 4-2 summarizes the islanding and non-islanding cases created for testing the proposed method.

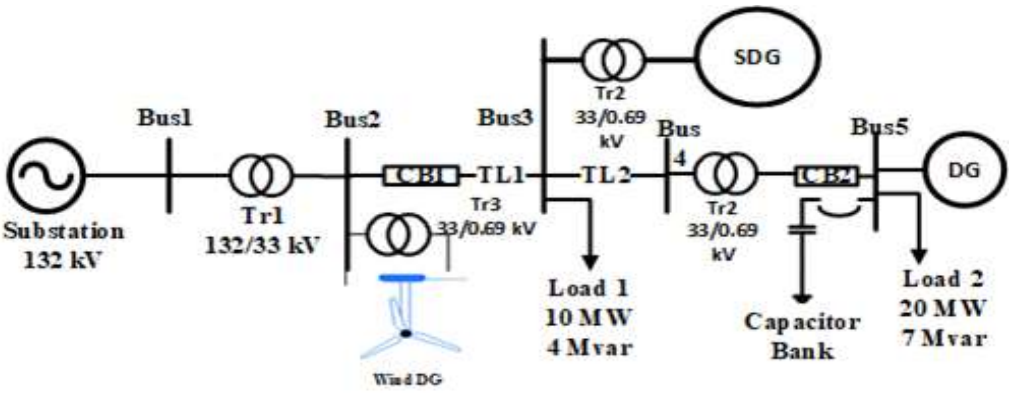

Figure 4.2 Single line diagram of Test system I

Table 4-2 Considered simulated test cases

No.	Types of Events	No. of test cases
1.	Islanding with different Mismatch i. Active power (0-15%) ii. Reactive power(0-20%)	100
Non-islanding		
2.	Capacitor bank (0.5-11.5 MVAR)	20
3.	Load shading (0-30 MVA)	30
4.	Fault (at Bus 2 & 5) with fault resistance(R_f) 0.01~100 ohm i. LG ii. LL iii. LLG iv. LLLG	100
5.	Induction Machine(IM) Starting (1~10 MVA)	10
6.	Reactor switching (0.5~9MVAr)	18

4.3.2 VMD based modal voltage decomposition under various test conditions

The captured voltage waveform at the PCC of the system under various operating scenarios has been acquired to obtain the modal voltage signal. Further, it has been processed through the VMD to extract the modes. In this section, the decomposition result of three cases has been analyzed.

1) Normal case

The modal voltage and decomposed modes have been depicted in Figure 4.3 (a) and (b). The first mode has the signal feature, while the remaining modes have negligible signal features, shown in Figure 4.3(b).

2) Capacitor switching event

The modal voltage during the capacitor switching event has been decomposed. The modal voltage and its modes are shown in Figure 4.4 (a) and (b). It has been observed in Figure 4.4. (b) that when the switching event occurs, its significant signature is present in mode2 and mode3.

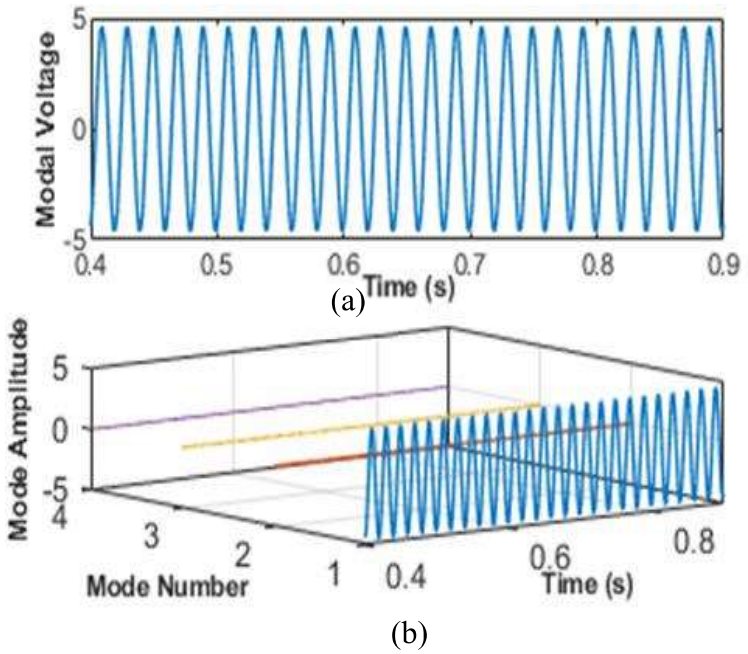

Figure 4.3 Non-islanding event (a) modal voltage (b) Decomposed signals

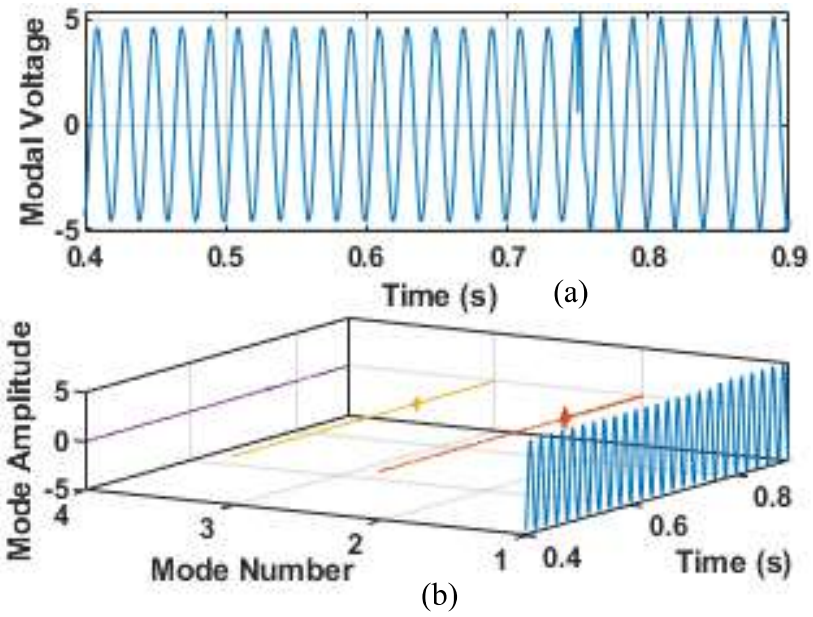

Figure 4.4 Capacitor switching case (a) modal voltage (b) decomposed signal

3) Islanding event

Figure 4.5(a) and (b) have inked the modal voltage and decomposed modes. In the case of the islanding event, mode2 has the dominant signature of this event, as shown in Figure 4.5(b). After analyzing the decomposition of these three cases', it is inferred that mode2 has the desired islanding signature, and hence it has been selected for mode energy index estimation.

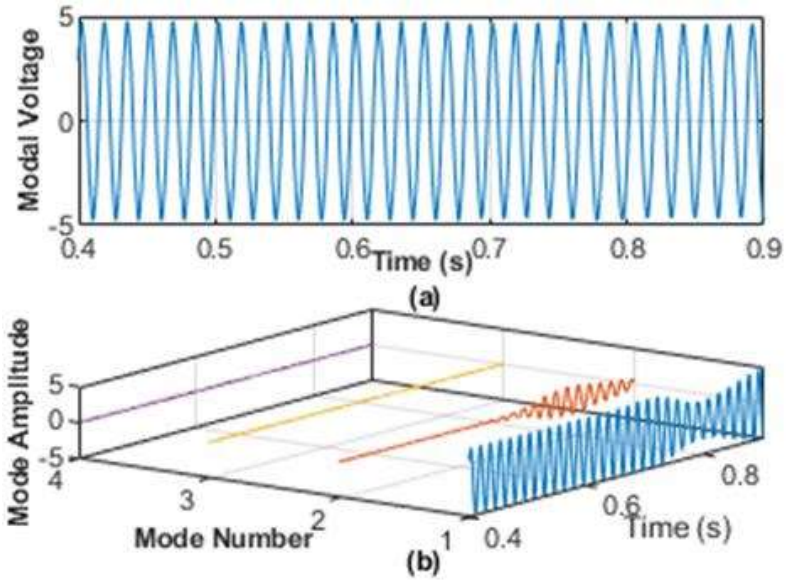

Figure 4.5 Islanding case (a) modal voltage (b) decomposed signal

4.3.3 Threshold selection

In this, the mode energy has been calculated at the targeted DG end, which has been chosen as an index to identify islanding events. As soon as the distribution system is islanded, a substantial change in mode energy is observed. However, the mode energy during non-islanding events does not change substantially. The change in mode energy varies from case to case. For precise discrimination between islanding and non-islanding events, a threshold has been selected after a large number of the experiment, including various non-islanding events such as dynamic load switching, capacitor switching, load

rejection, reactor switching, and islanding event with different active and reactive power mismatches. The threshold value is test system-dependent, which is denoted by the Energy Threshold (ET). Extensive simulations have been performed to distinguish between islanding and non-islanding events with appropriate distinction. The mode energy of the simulated events has been plotted for Test system I and Test system II (discussed in section 4.3.7) Figure 4.6. The mode energy of some critical cases of both test systems has been tabulated in Table 4-3. The maximum mode energy during LLLG fault in Test system-I is 68, and the minimum energy in case of islanding event with zero power mismatch condition is 73, as given in Table 4-3. So, the ET value of 70 has been selected for Test system-I. For Test system-II, the maximum mode energy for the non-islanding event is 32, and in the case of the islanding event's minimum energy is 35 during zero power mismatch conditions, as given in Table 4-3. The ET value of Test system II has been selected as 35.

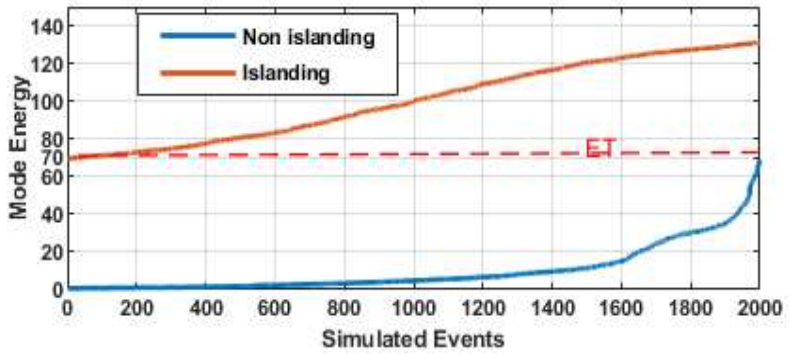

(a)

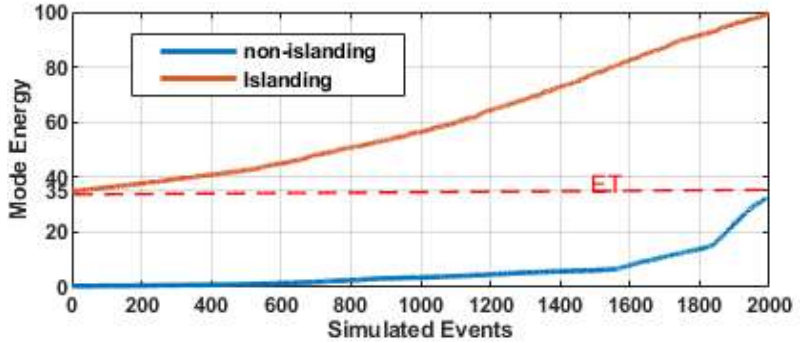

(b)

Figure 4.6 Mode energy of various simulated events for threshold selection in (a) Test system 1 (b) Test system II

Table 4-3 The mode energy of various critical cases of test systems

Sl.	Event	Energy(mode 2)	
Non-islanding cases		Test system-1	Test system-2
1.	Capacitor switching	18.1236 (11.5 MVAR)	15.21 (7 MVAR)
2.	IM starting (10 MVA)	0.1873	0.25
3.	LG fault at PCC (0.01 ohm)	1.6955	0.528
4.	LL fault at PCC (0.01 ohm)	13.796	0.5871
5.	LLG fault at PCC (0.01 ohm)	10.39	0.459
6.	LLLG fault at PCC (0.01 ohm)	68.02	31.8656
7.	Sag	0.3859	0.98
8.	Swell	0.3618	0.956
9.	Noise (SNR=20db)	0.6194	0.4272
10.	Load rejection	1.6684	1.24
11	Reactor switching	0.2526 (9MVAR)	0.1689(7MVAR)
Islanding cases			
11.	Zero power mismatch	73.96	35
12.	Subsequent capacitor switching and Islanding	132.74	272

4.3.4 Non-islanding event

In this section, various non-islanding events such as capacitor bank, load, reactor, and all types of fault events have also been simulated to authenticate the proposed IDT's effectiveness. The results are demonstrated in the following subsections.

4.3.4.1 *Capacitor, load switching events, and Reactor switching*

Capacitor banks are switched on and off frequently in the distribution system for power factor improvement. The proposed IDT's performance has been assessed with an 11 MVAr capacitor bank switching at 0.75s connected at bus three of Test system I to demonstrate the proposed method's ability. It is shown that the deviation in mode energy occurs at the instant of capacitor switching, as shown in Figure 4.7(a). The energy of mode2 is significantly less than ET at the capacitor's switching instant. The performance in the case of load switching at PCC has also been assessed. A subsequent load switching event of 33 % of the total load is disconnected at time 0.5 s and reconnected at time 0.55 s. Further, 66 % of the total load has been disconnected at 0.6 s and reconnected at

0.65 s. The mode energy plot in Figure 4.7(b) shows that load switching has less impact on the proposed method. In this series of events, the energy is lower than predefined ET $(i.e., 70)$ for islanding. The effect of load variation is negligible on the competency of the proposed scheme due to the lesser value of mode energy while load switching. Thus, the method is immune to the variation of loads.

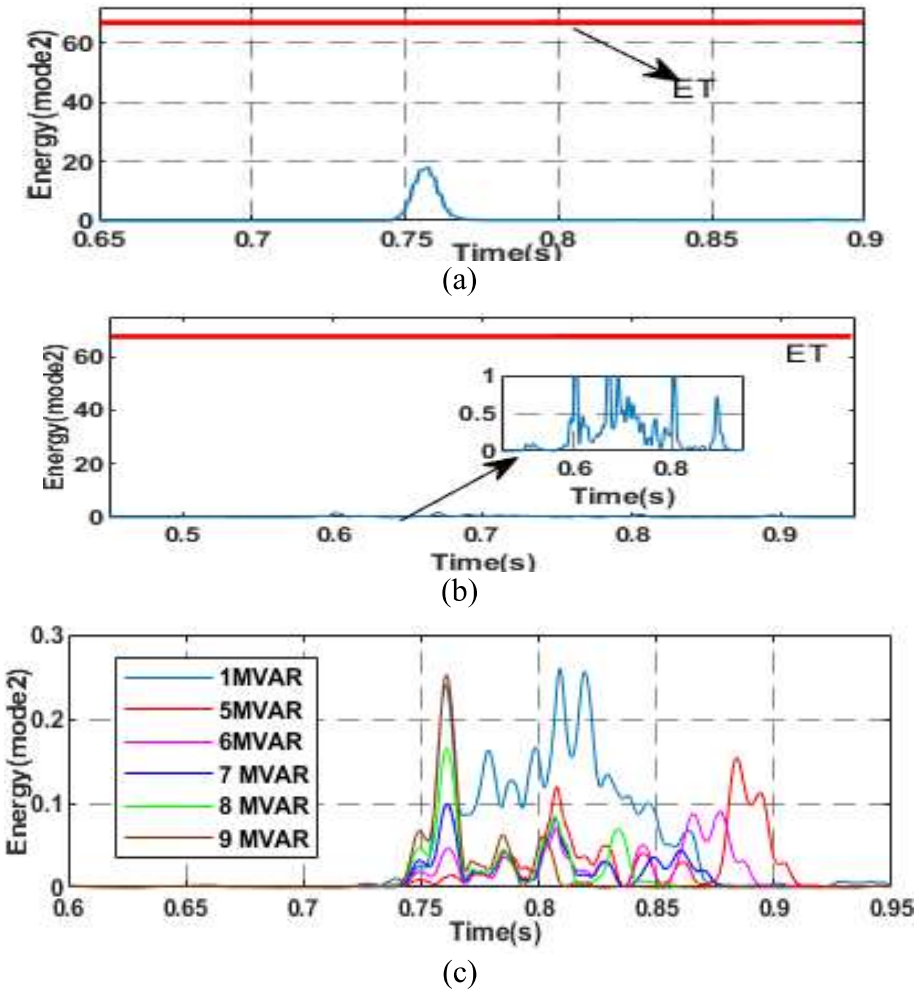

Figure 4.7 The energy of mode2 during (a) capacitor (b) subsequent load switching (c) Reactor switching

The reactor switching is a frequent event in case of lightly loading conditions to maintain voltage in limit. So to assess the performance of the proposed method, different ratings of reactor banks have been switched on at 0.75 s. The mode energy index for various events has been plotted in Figure 4.7 (c). It can be observed from the figure that

the reactor switching has significantly less impact on mode energy. This reaffirms that the proposed method efficiently distinguished it as a non-islanding event.

Based on the results obtained, it can be comprehended that the mode energy index is highest in the case of capacitor switching, least in the case of reactor switching. On the other hand, it is between the capacitor and reactor switching in case of load switching.

4.3.4.2 *Fault events*

During the fault events, the relaying system should effectively classify an event with clear fault discrimination as a non-islanding scenario preventing false DG tripping. IDT presented in this work has been tested for its efficacy under multiple fault conditions in Test system I. To investigate the impact of fault events, multiple cases, including single-line-to-ground (LG), double line to line (LL), double-lines-to-ground (LLG), and three-lines-to-ground (LLLG) faults at varying locations and different fault resistances have been simulated. The critical results that significantly impact the mode energy have been discussed in this section. The inception of the fault has been set at 0.75s of 0.05s duration. The fault resistance (R_f) is 0.01 ohm in all these fault events. The plot of the energy corresponding to $mode\ 2$ has been inked in Figure 4.8(a) and Figure 4.8(b), with the former containing the signature captured at PCC for fault taking place at bus 2, while the letter shows the signature for fault at PCC.

It can be inferred from the depicted plots that: -

i. The mode energy is lower when the fault does not occur at PCC.
ii. Although mode energy is higher in the case of fault at PCC, the mode energy remains below the set threshold value (ET), discriminating the islanding and non-islanding events.

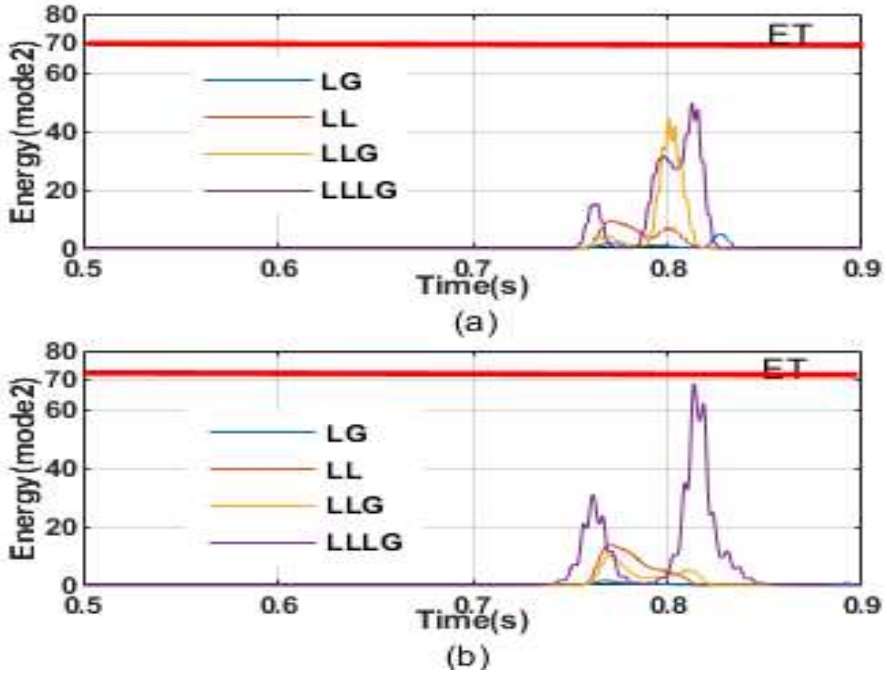

Figure 4.8 The mode energy of signal for various fault conditions (a) fault at bus2 (b) fault at PCC

4.3.4.2.(i) High impedance fault (HIF)

The efficacy of the proposed IDT has been thoroughly assessed for HIF and LIF events. The two different locations of the Test system, I have been subjected to high impedance fault (850 to 1000 ohm) [100]. The results are shown in Figure 4.9(a). From the Mode energy, it would be concluded that the HIF has no significant impact on the proposed method. The mode energy during HIF has been well below the ET.

4.3.4.2.(ii) Low impedance fault(LIF)

The LIF event (1 to 100 ohm) [100] has been simulated at two locations. The result is shown in Figure 4.9(b) shows that the LIF has a significant impact on mode energy. Therefore, it has easily been discriminated as a non-islanding event by the proposed method. The results of different LIF(1~100 ohm) have been depicted in Figure 4.9(b).

Hence, it has been reaffirmed that the proposed IDT is well effective in discriminating between islanding and faults events during varying scenarios.

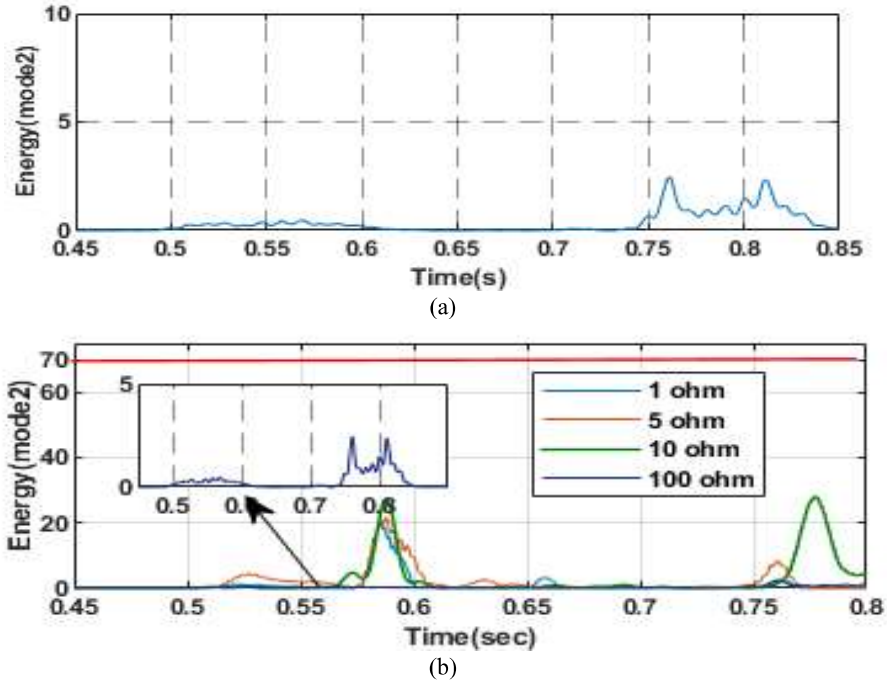

Figure 4.9 The mode energy of signal (a) HIF (b) LIF

4.3.4.3 *Sag and Swell event:*

The proposed scheme's effectiveness during critical power quality issues has also been evaluated. The voltage signal has been subjected to sag and swell conditions at 0.5 s to 0.7 s. The computed mode energy index has been plotted in Figure 4.10. The mode energy is significantly less compared with predefine ET. So, this event has been easily distinguished as non-islanding by the proposed method.

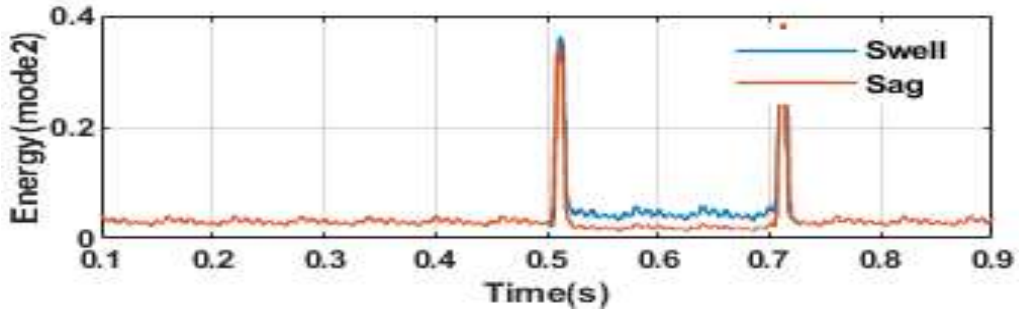

Figure 4.10 The mode energy of signal during Sag and Swell events

4.3.4.4 *Effect of noise disturbance*

The voltage signal contaminated with noise is also considered during the efficacy check of the proposed IDT. Generally, the signal-to-noise ratio (SNR) is 20-45 dB in practice. The noise signal is mixed with the voltage waveform, and it is processed with VMD to obtain decomposed modes. The mode energy has been plotted as shown in Figure 4.11, respectively. The results show that mode energy is significantly less than predefined ET. It clearly vindicates that the proposed method is effective in noisy environments.

4.3.4.5 *Induction machine switching events:*

The impact of induction machine load on voltage waveform during switching transient has also been assessed. A 10 MVA rated IM has been connected at $t = 0.75\ s$ at PCC. The modal voltage waveform captured at PCC is shown in Figure 4.12(a). It is observed that a slight dip in the voltage waveform has been observed during the induction machine switching. There is a minor variation in the mode energy at the time of switching, depicted in Figure 4.12(b). Thus, starting transient and islanding events can be easily discriminated by the proposed method.

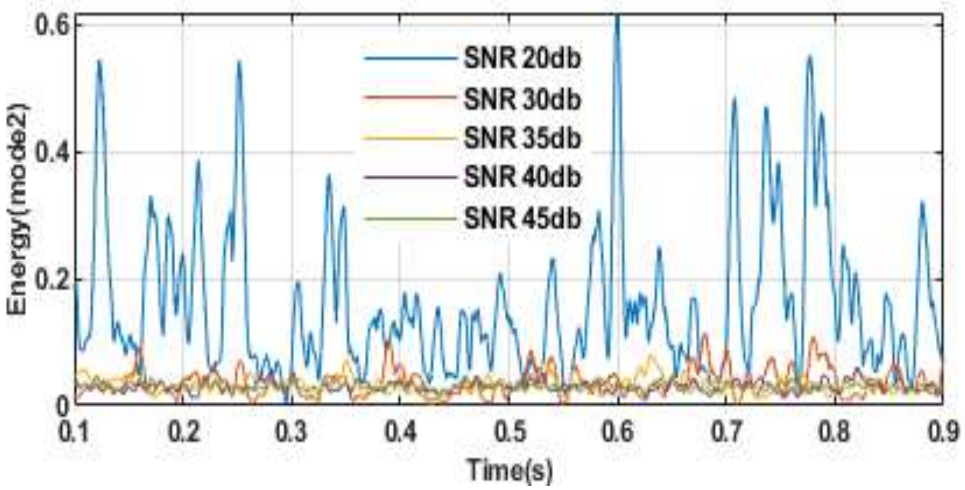

Figure 4.11 The mode energy of signal during noise disturbances SNR ratio (20,30,35,40 and 45 dB)

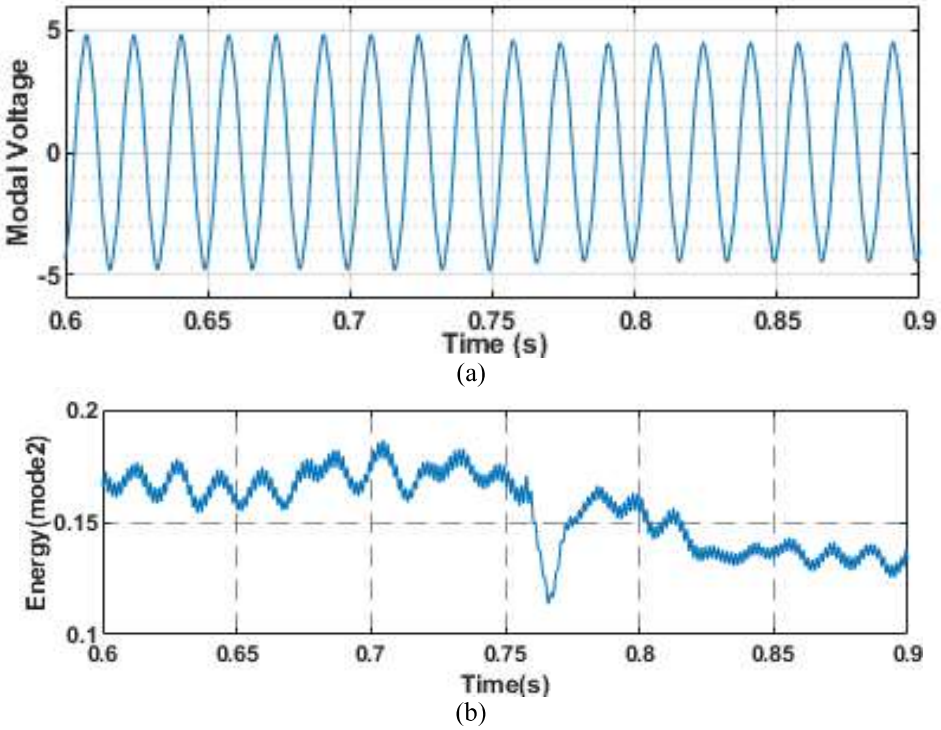

Figure 4.12 Performance of purposed IDT during IM starting (a) modal voltage (b) energy of mode2

4.3.5 Islanding event

When a portion of the distribution system is isolated from the primary grid and the DG system is still energized, the event is referred to as an islanding event. The islanding scenario has been simulated through opening circuit breaker CB1 of the test system inked in Figure 4.2. The breaker operates at 0.68s disconnecting the circuit. The islanding event is having an impact on the DG end voltage. Therefore, the voltage's modes would contain the islanding incident's signature as the grid isolates from the system. However, it is complicated to identify the voltage signal change in less power mismatch conditions. In this section, different types of active power mismatch (APM) and Reactive power mismatch cases have been simulated by opening the CB1, and the performance of the proposed IDT has been thoroughly evaluated.

4.3.5.1 *Zero power mismatch (ZPM):*

When power flow from the grid to the PCC is nearly zero, it poses a challenge to detecting islanding for the conventional relays because of its large NDZ. However, the proposed technique effectively identifies islanding events during zero deficit active power conditions, as shown in Figure 4.13(a). The islanding is incepted at $t = 0.68s$ and the mode energy has crossed the threshold at the time instant $t = 0.79s$ as shown in Figure 4.13(a). The time taken to cross the threshold is $0.11s$.

4.3.5.2 *Active Power Mismatch (APM):*

The proposed IDT has been evaluated for different APM values between the grid and the DG system in the islanding case. The power mismatch has been defined as the shortage of power delivered to the system by the utility grid and the DG to satisfy the distribution network's load demand. The different APM values ($i.e., \pm 5\%\ to\ \pm 15\%$) are created by varying the PCC load. The islanding scenario has been created at $t = 0.7\ s$ for two different values of the APM. The proposed IDT's mode energy results for $\pm 5\%\ to\ \pm 15\%$ APM are depicted in Figure 4.13(b). The result shows that VMD's mode energy index crosses the ET threshold level, ascertaining the islanding events with different APM conditions. Hence, it has been reaffirmed that the proposed IDT can precisely detect the islanding event for any APM value effectively.

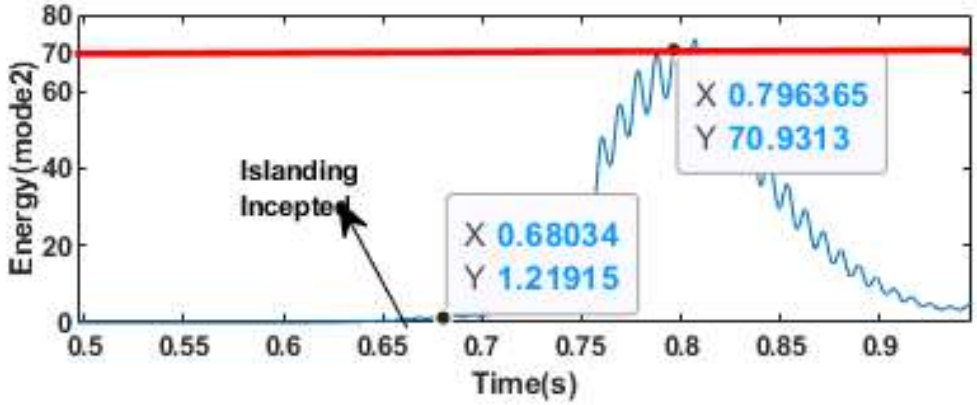

(a)

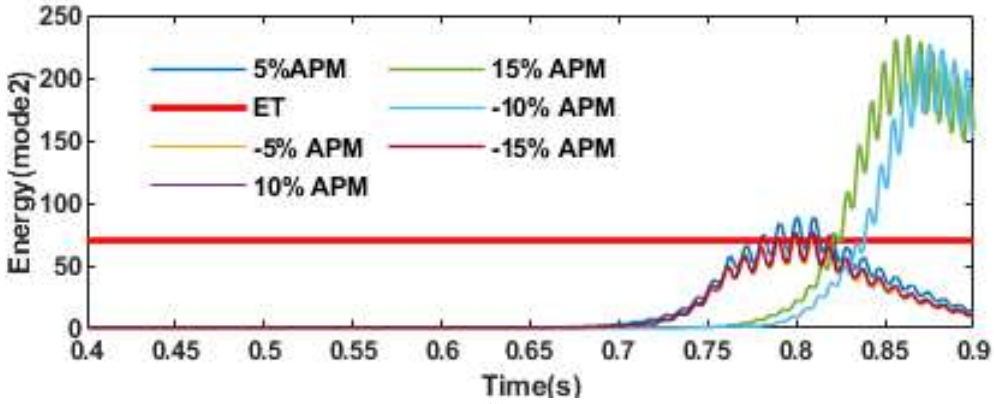

(b)

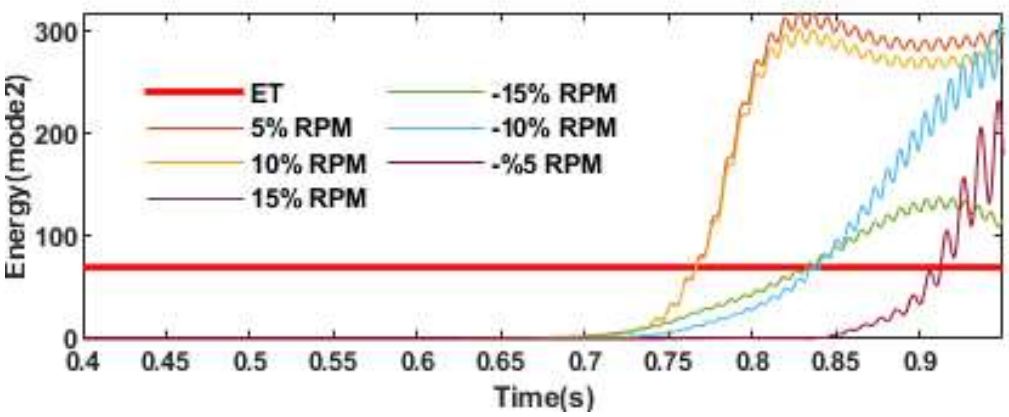

(c)

Figure 4.13 The mode energy plot in (a) zero power mismatch (b) active power mismatch (c) reactive power mismatch

4.3.5.3 *Reactive Power Mismatch (RPM):*

In this islanding case, the proposed IDT has been assessed for different RPM values $(i.e., \pm 5\% \; to \; \pm 15\%)$ between the DG and the main grid. The islanding scenario has been created at $t = 0.7\,s$ for two different values of the RPM. The proposed IDT's performance is shown in Figure 4.13(c). The mode energy plot shows that the energy

index for different RPM values crossed the threshold ET, ensuring the proposed IDT can identify the islanding event for minimal RPM values.

4.3.5.4 *Impact of DG Type on Islanding Detection*

Different types of DG, such as PV, Synchronous, and Wind (DFIG) have been considered to validate the proposed IDT. The energy index of mode 2 after islanding under different target DG has been shown in Figure 4.14. The islanding incepted at 0.7 s considers SDG as a target DG, and the ET crossed at 0.8 s. While considering PV and wind type DG as target DG with islanding inception at 0.75 s, the ET crossed at 0.87 s and 0.84 s, respectively. In all the cases, active and reactive power mismatches are considered to be within $\pm 5\%$.

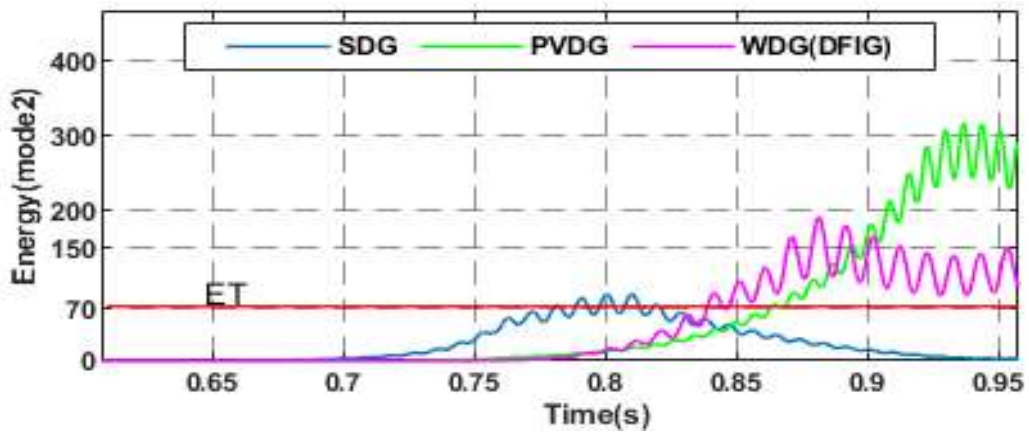

Figure 4.14 Mode energy plot for different types of DG in case of Islanding

4.3.6 Analysis of NDZ for proposed IDT

The quantification of the islanding protection performance is done through the NDZ index [101] by varying shapes of NDZ obtained for different DG. For synchronous generator-based systems, reactive power imbalance influences the NDZ. In such cases, it (reactive power imbalance) also defines the top and bottom boundaries (i.e., the ordinate of the plot), along with the active power imbalance level (i.e., abscissa of the plot). The

effect of active power mismatch is dominant in frequency function performance and is a determinant for the left and right boundaries. The power imbalance equation (4.4) and (4.5) are taken from [101]. The power imbalance (measured at distribution system PCC) drives the performance index that has been plotted in ΔP–ΔQ space, as shown in Figure 4.15. In the case of inverter-based systems, NDZ's size depends on the inverter control topology.

$$\left(\frac{V}{V_{max}}\right)^2 - 1 \leq \frac{\Delta P}{P} \leq \left(\frac{V}{V_{min}}\right)^2 - 1 \qquad 4.4$$

$$Q_f\left(1 - \left(\frac{f}{f_{min}}\right)^2\right) \leq \frac{\Delta Q}{Q} \leq Q_f\left(1 - \left(\frac{f}{f_{max}}\right)^2\right) \qquad 4.5$$

where V_{max} is the maximum limit of over-voltage, V_{min} is the minimum limit of under-voltage, f_{max} is the maximum limit of over frequency, f_{min} is the minimum limit of under frequency, Q_f is the quality factor, V is the rated voltage, f is the rated frequency, P is the active power, Q is the reactive power, ΔP is the active power mismatch, and ΔQ is the reactive power mismatch. The conventional relay power mismatch is given $-17.35\% \leq \Delta P \leq 29.13\%$ and $-5.94\% \leq \Delta Q \leq 4.11\%$. The proposed IDT ΔP *and* ΔQ was found to be less than 1% during simulation analysis.

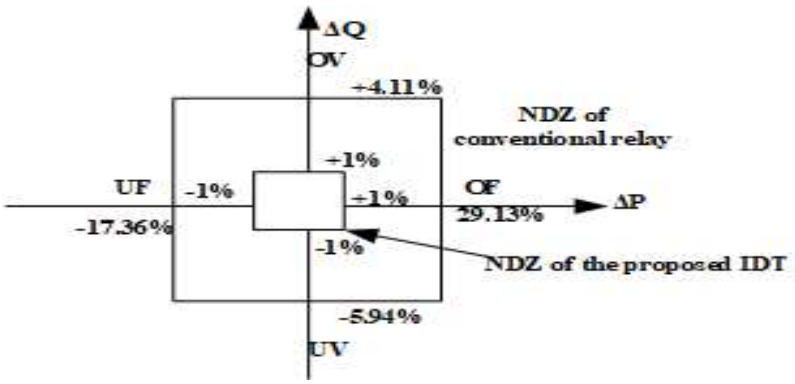

Figure 4.15 Comparision of NDZ of the proposed IDT with conventional relays (over-voltage /frequency and under-voltage/frequency)

4.3.7 Test system II:

Validation of the proposed IDT has been done through its implementation on the part of the practical distribution network of Madhya Gujrat, India [102]. A single-line diagram depicting the above-mentioned system is shown in Figure 4.16. The system has been modified by incorporating 3 DGs in the system. Two of the DG's, DG1 and DG3 (synchronous generator type), are connected to 11 kV bus, DG1 being at PCC and DG3 connected through feeder 4 (TL4). Inverter type photovoltaic (PV) DG2 is connected at feeder eight. The modeling parameters of load, transformers, and transmission line details are taken from [102], while the parameters of DG have been given in the appendix. Multiple faults, islanding, and other critical scenarios (such as sag, swell, and capacitor switching) have been simulated and tested. Various islanding and non-islanding events (400 events) have been generated and tested during the investigation.

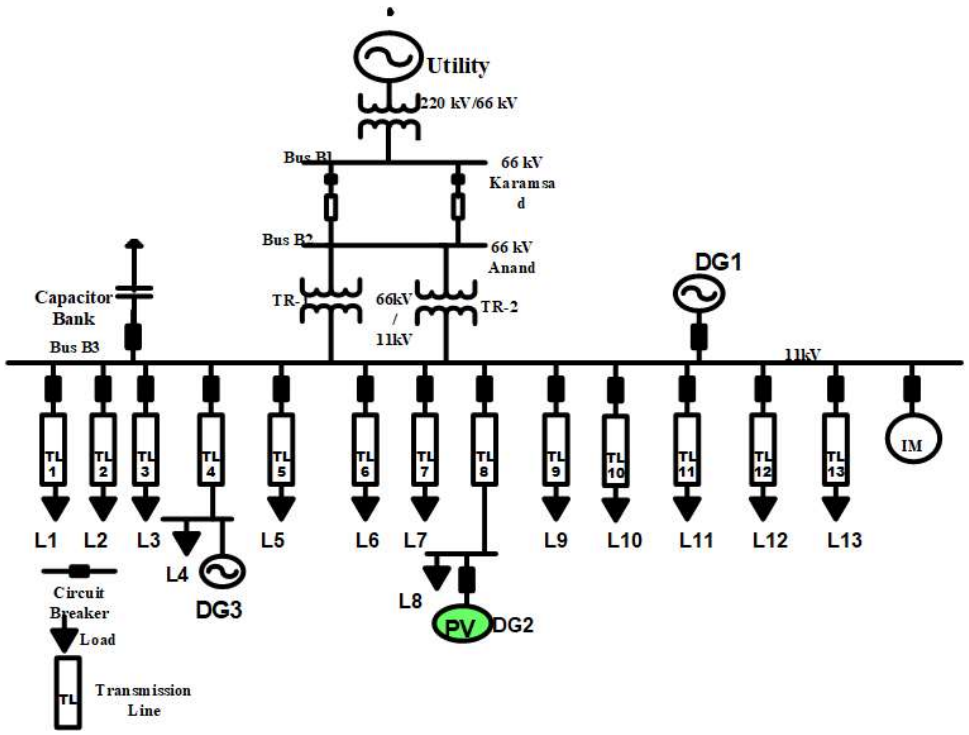

Figure 4.16 One-line diagram of Test system-II [102]

Some critical results have been described in this section to show the proposed method's performance during critical islanding and non-islanding events.

4.3.7.1 *Various non-islanding:*

The mode energy index has been depicted in Figure 4.17(a) for three phases to ground fault. The results clearly show that the mode energy is below the threshold value, and the method is correctly classified into non-islanding. The mode energy plots for various non-islanding events have been shown in Figure 4.17 (b). In all the non-islanding events, the mode energy has been below the ET values. So, this method successfully discriminates between islanding and non-islanding events.

4.3.7.2 *Islanding events:*

The mode energy index in the case of various islanding events has been shown in Figure 4.17 (c). The mode energy index has crossed the energy threshold for various reactive and active power gap scenarios. The zero-power deficit scenario crosses the predefined threshold values, and the islanding event is successfully identified.

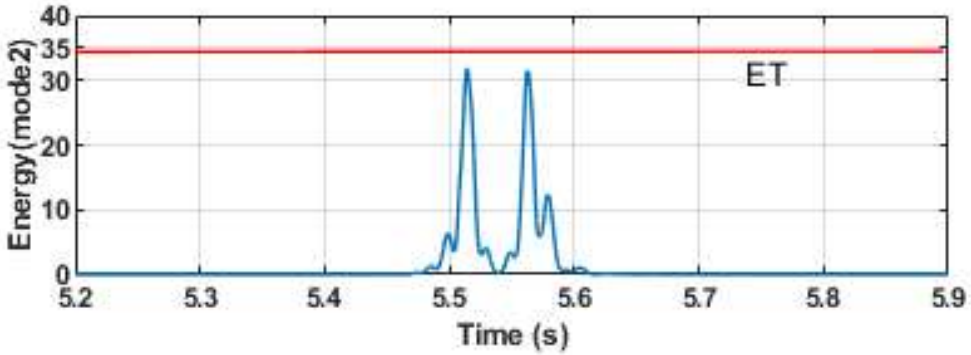

(a)

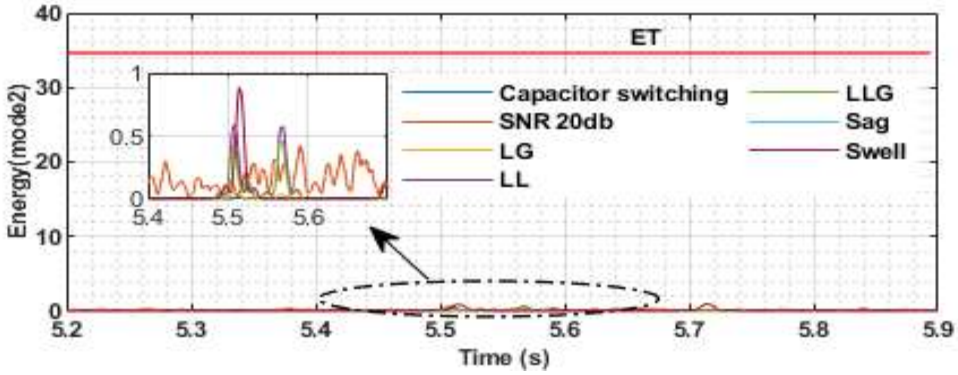

(b)

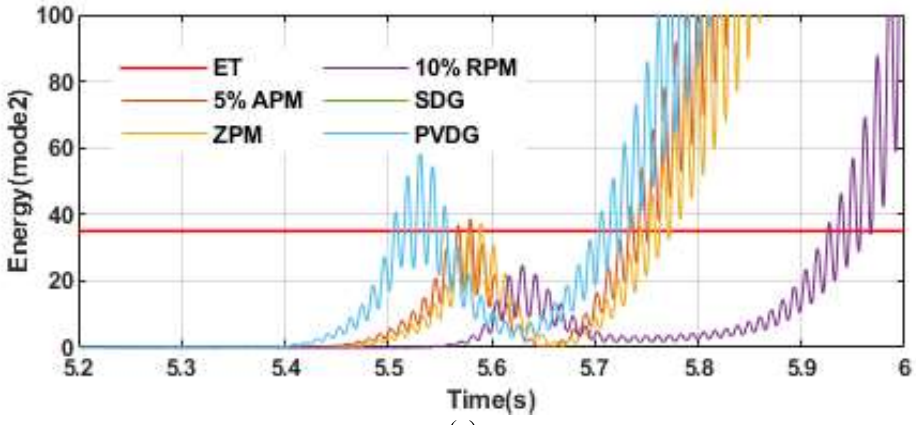

(c)

Figure 4.17 The energy of mode2 for Test system II (a) LLLG (b) different non-islanding events, (c) Islanding conditions at different power mismatch conditions

4.4 COMPARATIVE ASSESSMENT OF THE PROPOSED IDT WITH EXISTING METHODS

This subsection has thoroughly described the comparative assessment of feasibility and competency of the proposed IDT mechanism in terms of NDZ, response time, and variation of DERs. The comparative analysis of the proposed approach with previously available techniques has been tabulated in Table 4-4. In Ref.[103], the application of

ROCOF and vector surge relay for synchronous type DG has been reported. However, its significant limitations are the dependency of tripping time on power mismatch and relay setting on the inertia constant of the synchronous generator. The relay may not trip even in the case of islanding if the power imbalance is small. The conventional relay [104] has larger NDZ and is inappropriate for islanding where power deficits are small. In addition, active ROCOF based IDT continuously injects disturbance signal in the system, making it unsuitable for SG types DG. Ref.[105]-[106] reported IDT methodologies for nearly zero power mismatch cases. However, the approach has not been assessed for inverter type DG. Ref. [107]-[108], have considered only inverter type DG for efficacy assessment, but both have a higher response time. Similarly, [109] has considered only wind and SG type DG but has a larger detection time. In addition, it requires extensive training and testing data. Ref.[110] has reported an active IDT, but it has only considered inverter type DG during testing. Ref.[56] has considered all types of DGs during testing. However, its implementation is very intricate as it utilizes TVF based EMD decomposition and Teaser energy operator, which may not be suitable for real-time applications. The proposed approach has also been assessed for all types of DG, i.e., inverter, wind (DFIG), and SG-based DGs. It can easily be observed from Table 4-4 that the proposed IDT approach overcomes all the limitations as mentioned earlier with better time response capability. In addition, the proposed IDT has been validated in a Real-time environment as described in next section. Moreover the proposed IDT is a passive method, so it does not affect the system's power quality.

Table 4-4 Comparison of recent IDT with the proposed method

IDT method reported	Power mismatch($\Delta P/P_{DG}$)	Detection time	DG type		
			PV (inverter type)	Wind (DFIG)	SG
Ref.[35]	≈ 0	≤100 ms	×	✓	×
Ref.[103]	≈ 18	≥200 ms	×	×	✓
Ref.[56]	≈ 0	≤15 ms	✓	✓	✓
Ref.[104]	-29 to 17	≤ 2 s	×	×	✓
Ref.[105]	≈ 0	≤ 201 ms	×	×	✓
Ref.[106]	= 0	≤66 ms	×	×	✓
Ref.[107]	≈ 0	≤ 60 ms	✓	×	×
Ref.[108]	= 0	≤ 60 ms	✓	×	×
Ref.[109]	≈ 0	≤ 744 ms	×	✓	✓
Ref.[110]	≈ 0	≤ 200 ms	✓	×	×
Proposed IDT	≈ 0	≤ 0.11s	✓	✓	✓

4.5 VALIDATION IN REAL-TIME USING REAL-TIME DIGITAL SIMULATOR (RTDS) PLATFORM

The realization of the proposed IDT has been carried out on RTDS/RSCAD simulator [111]. Test System II has been modeled in RSCAD/RTDS environment. The simulator consists of NovaCor chassis with four licensed cores and RSCAD 5.013 versions. The simulation is performed in Power system mode, having a solution time step of 50 microseconds. NovaCor chassis has 12 × 12 bit digital to analog channels (GTAO) operating over a range of ±10 V peak. The PCC three-phase voltage has been sent from the front panel interface of RTDS (GTAO) to MicroLabBox (dSPACE1202) [112] ADC pin where the proposed algorithm has been implemented. The modal voltage has been decomposed, and the energy of the second mode is computed. The computed energy is compared with the threshold value. In case it is greater than the predefined threshold, a trip signal is generated and sent to RTDS by the GTNET-SKT communication protocol.

The schematic arrangement of the Real-Time Simulation Platform has been shown in Figure 4.18.

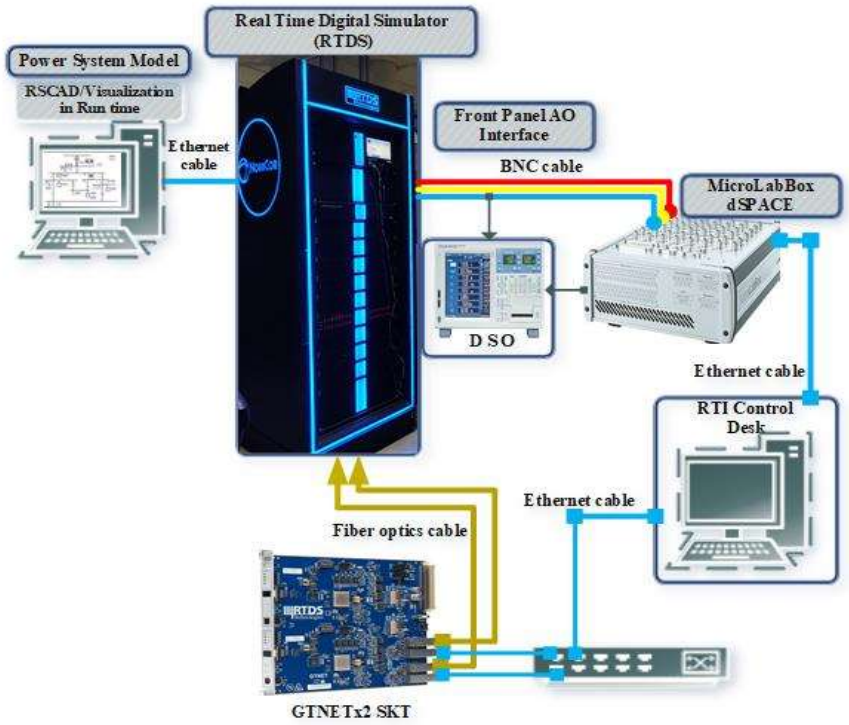

(a)

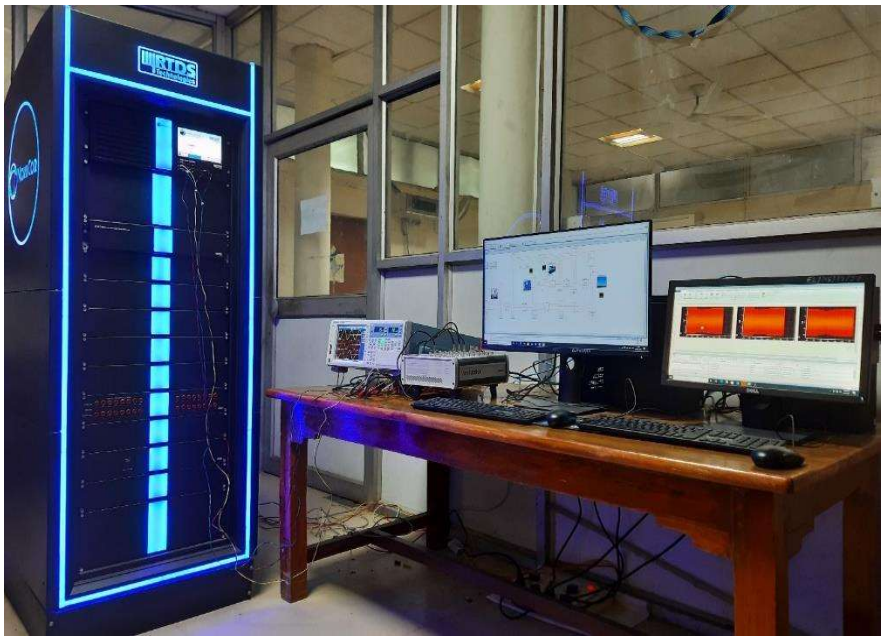

(b)

Figure 4.18 Real-time simulation platform for the implementation of the proposed IDT (a) Block diagram (b) Laboratory setup

In the following subsection, the results are presented, and a discussion on the various non-islanding and islanding events is presented for authenticating the proposed IDT.

4.5.1 Non-Islanding cases

4.5.1.1 *Subsequent capacitor switching*

For power factor correction in the distribution system, capacitor banks are widely used. It introduces switching transient into the system, so identifying this switching event with an islanding scenario is vital in any islanding protection scheme. The presented IDT performance during switching of capacitor bank with full load has been assessed and plotted in Figures 4.19(a) and (b). Figure 4.19 (a) shows that during subsequent switching of three 0.5 MVAr capacitor banks connected at PCC, the mode energy magnitude is significantly less than the threshold energy (ET).

In Figure 4.19(b), a 1.5 MVar capacitor bank is switched on in one case. It has been seen that the mode energy is well below the ET. Hence, the presented algorithm remains stable during the switching of capacitor banks.

4.5.1.2 *Faults on Distribution Feeder:*

The IDT presented in this article has been evaluated under different fault types at different locations on the Test system-II. The performance of the proposed IDT is shown in Figure 4.19(b). It is observed that the proposed IDT has a sufficient margin of ET in case of fault events occurring in the system. The LLLG has maximum mode energy, and it is well below the threshold, as seen in Figure 4.19 (b).

4.5.2 Islanding Situations

The performance of the presented method has been assessed during actual islanding events. The performance during islanding events with 10% active and reactive power

mismatch conditions has been shown in Figure 4.19(c). It has been observed that after islanding, the mode energy crosses the threshold value. The islanding situation with a 0% active power mismatch condition has exceeded the threshold value shown in Figure 4.19(d). The competency of the proposed method in a Real-time simulation environment for multiple islanding and non-islanding events is thoroughly investigated. The proposed method effectually distinguished the islanding events from other non-islanding events with sufficient margins in transients' events.

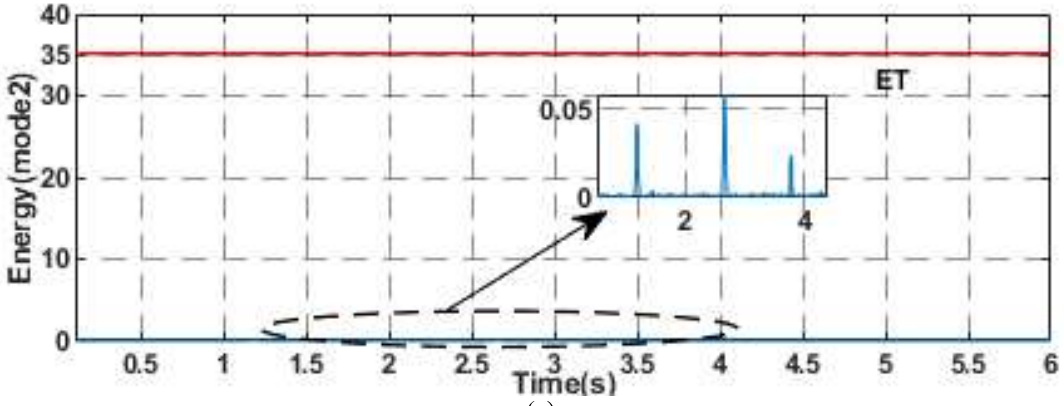

(a)

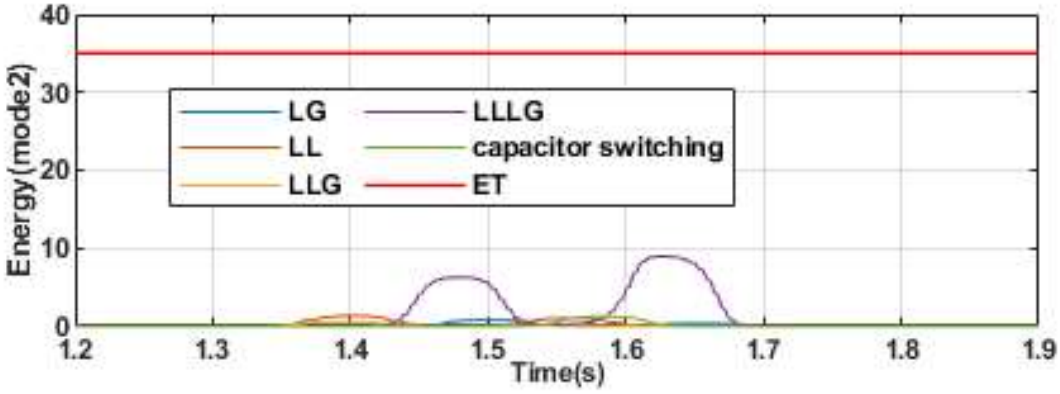

(b)

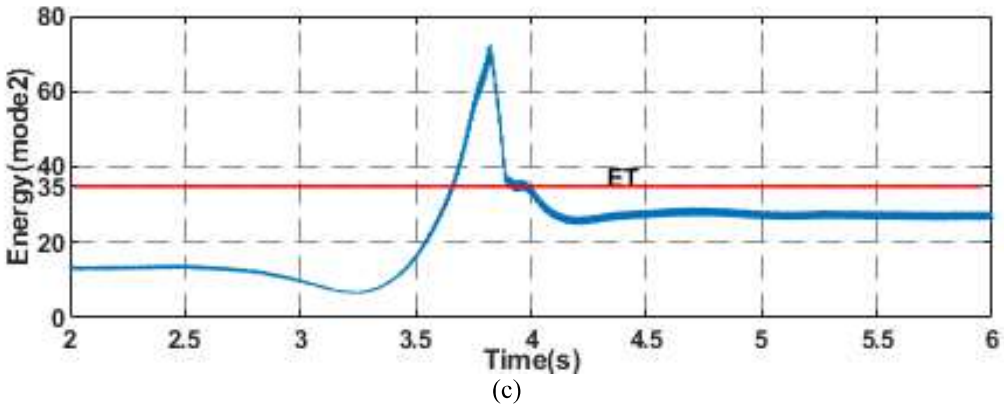

(c)

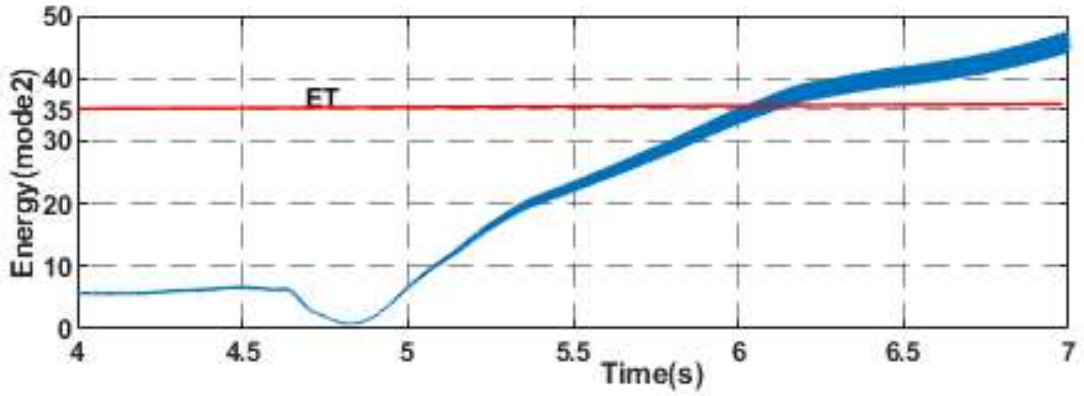

(d)

Figure 4.19 Performance of the purposed IDT in RTDS platform (a) subsequent capacitor banks on and off (b) different types of faults events (c) Islanding event (d) Islanding and capacitor switching simultaneously.

4.6 SUMMARY

The real-time implementation of the proposed modal voltage decomposition-based passive method has been presented using RTDS/RSCAD and Microlab box. It utilizes the VMD to extract the four modes from the modal voltage signal. The energy index of the second mode has been opted to discriminate islanding events. The proposed IDT's performance has been substantiated by testing it on two different test systems under various operating scenarios. The simulation results reveal that the proposed IDT precisely identifies islanding events under critical power mismatch conditions. The proposed method's prime attribute is its performance under the voltage signal contaminated by external noise and faster time response. Moreover, it has systematically mitigated NDZ. Further, the effectiveness of the proposed scheme has also been validated on a practical distribution network in the presence of multiple DGs. The simulation results reaffirmed that IDT is proficient in detecting the islanding events. Further, the proposed method is validated on a real-time simulation platform RTDS and dSPACE to establish its feasibility in a Real-world environment.